Optical Engineering

OpticalEngineering.SPIEDigitalLibrary.org

Imaging of high-pressure fuel sprays in the near-nozzle region with supercontinuum illumination

Yipeng Zheng
Jinhai Si
Wenjiang Tan
Mingxin Wang
Bo Yang
Xun Hou

SPIE.

Yipeng Zheng, Jinhai Si, Wenjiang Tan, Mingxin Wang, Bo Yang, Xun Hou, "Imaging of high-pressure fuel sprays in the near-nozzle region with supercontinuum illumination," *Opt. Eng.* **57**(4), 043114 (2018), doi: 10.1117/1.OE.57.4.043114.

Downloaded From: https://www.spiedigitallibrary.org/journals/Optical-Engineering on 5/7/2018 Terms of Use: https://www.spiedigitallibrary.org/terms-of-use

Imaging of high-pressure fuel sprays in the near-nozzle region with supercontinuum illumination

Yipeng Zheng,[a,b] Jinhai Si,[a,b,*] Wenjiang Tan,[a,b] Mingxin Wang,[a,b] Bo Yang,[a,b] and Xun Hou[a,b]
[a]Xi'an Jiaotong University, School of Electronics and Information Engineering, Key Laboratory for Physical Electronics and Devices of the Ministry of Education, Xi'an, China
[b]Xi'an Jiaotong University, Shaanxi Key Lab of Information Photonic Technique, Xi'an, China

Abstract. We employ a supercontinuum (SC) illumination to image the high-pressure fuel sprays in the near-nozzle region. The effect of speckles in the images is significantly mitigated using the SC illumination to improve the identifiability of the microstructures in the spray. The microstructures in the near-nozzle region, i.e., lobes, holes, ligaments, and bridges, are clearly imaged for different fuel pressures and nozzle orifice diameters. The shadowgraphs captured in the experiments also show the spray cone angle of spray is strongly dependent on the injection pressures and nozzle orifice diameters. © *2018 Society of Photo-Optical Instrumentation Engineers (SPIE)* [DOI: 10.1117/1.OE.57.4.043114]

Keywords: supercontinuum; spray; near-nozzle region; speckle.

Paper 172016 received Dec. 19, 2017; accepted for publication Apr. 16, 2018; published online Apr. 28, 2018.

1 Introduction

The liquid surface shapes of high-pressure fuel sprays in the near-nozzle region show the smaller structures on the conical spray core, i.e., holes, bridges and ligaments, which are the precursors to droplet and spray formations.[1,2] For optimizing the injection process to increase fuel combustion efficiency and reducing pollutants emission, it is critical to study the primary breakup of the liquid core in this region.[3–6] During the last decade, great efforts have been devoted to record the images of the high-velocity fuel spray in the near-nozzle region using lasers.[7–10] However, high photon degeneracy of the lasers leads to speckles that originate from the random interference due to multiple light scatterings from surrounding liquid droplets. The speckle patterns appear as additional features that are not present in the fuel spray and, thereby, corrupt the identifiability of spray features. If speckle formation could be prevented, the spray image clarity would be improved. Speckles can be mitigated by generating and averaging multiple uncorrelated speckle patterns on an irradiance basis (for instance, by introducing time-varying local phase shifts within the light beam illuminating the sample).[11] Unfortunately, to image rapid transients in fuel spray, it is impossible to generate multiple uncorrelated speckle patterns for its necessary forming time. Another method to reduce speckle noise is based on image-processing techniques.[12] However, this method may lose the spray features information that was corrupted due to speckles; rather, they merely mitigate the speckle effects.

In the past few years, there has been considerable interest in the application of incoherent laser sources to fundamentally preclude the formation of the speckles. When illuminating with a low-coherence source, speckle noise is suppressed to be a uniform background. Redding et al.[13,14] demonstrated that lasers with low spatial coherence, e.g., random lasers and chip-scale electrically pumped semiconductor lasers, can be engineered to provide speckle-free imaging in intense optical scattering conditions. Cui et al.[15] resolved the issue of the speckle using a method of wavelength modulation to reduce the temporal coherence of the laser. In the last two decades, femtosecond lasers have been reported as a promising tool for laser processing and ultrafast measurements.[16–19] As a new illumination source, the supercontinuum (SC) induced by a femtosecond laser has found numerous applications in many diverse fields, including spectroscopy,[20] fluorescence imaging,[21] and optical coherence tomography.[22] Because of its spectrum broadening, leading to temporal coherence degeneration,[23] SC can be used as the illumination source to suppress the effect of speckles for imaging in a scattering environment.[24,25] And due to its temporal ultrashort pulse width, SC may be an ideal illumination source for imaging the high-speed fuel sprays in the near-nozzle region to avoid producing motion blurring effects.

In the study described herein, we employ SC illumination to image high-pressure fuel sprays in the near-nozzle region. Using SC illumination, we significantly mitigate the effect of speckles in the images to improve the identifiability of the microstructures in the sprays. High fuel pressures (P_r) in a range from 200 to 1200 bar and nozzle orifice diameter (d) ranging from 80 to 180 μm are implemented. The microstructures in the near-nozzle region, i.e., lobes, holes, ligaments, and bridges, are clearly imaged under different fuel pressures and nozzle orifice diameter conditions. The shadowgraphs captured in the experiment also show the spray cone angle of spray to depend on these injection conditions.

2 Experiment

Figure 1 shows the experimental setup scheme for imaging fuel spray using SC illumination. A Ti:sapphire laser system (Libra-USP-HE, Coherent Inc.), which can generate 800-nm

*Address all correspondence to: Jinhai Si, E-mail: jinhaisi@mail.xjtu.edu.cn

0091-3286/2018/$25.00 © 2018 SPIE

Downloaded From: https://www.spiedigitallibrary.org/journals/Optical-Engineering on 5/7/2018 Terms of Use: https://www.spiedigitallibrary.org/terms-of-use

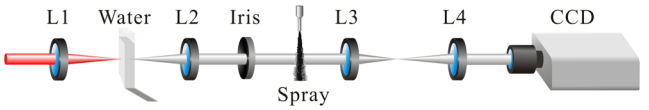

Fig. 1 Schematic diagram of imaging using SC illumination. L1, L2, L3, and L4: lenses.

laser pulses with widths <50 fs and energies of about 3.5 mJ per pulse at a repetition rate of 1 kHz, is used in our experiments. As shown in Fig. 1, the femtosecond laser pulses are focused by lens L1 (focal length, $f_1 = 150$ mm) inside a 5-cm-thick quartz cuvette filled with distilled water to generate the SC. The pulse width of the SC is measured to be about 1.5 ps. The generated SC is collected by lens L2 ($f_2 = 100$ mm) and transmits the near-nozzle region of fuel spray. The transmission light is collected by lens L3 ($f_3 = 160$ mm), which is placed at f_3 from the object plane. The light pulse is imaged by a lens L4 ($f_4 = 200$ mm) onto a charge-coupled device (CCD) camera (INFINITY3-1M-NS-TPM, Lumenera Corporation, Canada) with 1-ms exposure time.

In this experiment, the diesel is delivered by a high-pressure diesel fuel pump (CP3.3N, BOSCH, Germany) driven by an electric motor to a single-orifice, common-rail diesel injector (CRIN2-16, BOSCH, Germany) to generate spray; d of the injector ranges from 80 to 180 μm and the orifice length is 170 μm. An integrated electrical controller (OD2302, Power MAC, China) is used to adjust the time delays and duration of the injector jet. When the injector sprays, the controller triggers the CCD camera to ensure that it obtained an image simultaneously to catch the moment at which the spray began. Moreover, the controller is used to change the P_r from 200 to 1200 bar under each nozzle diameter condition by modifying the load on the electromagnet in the pump.

3 Results and Discussion

A US Air Force resolution target (RT-MIL-TP2001, RealLight, China) is used as the object to characterize the identifiability of the images. As shown in Figs. 2(a) and 2(b), we, respectively, capture the images of the test patterns without scattering medium using the 800-nm femtosecond laser and SC illuminations as described in Fig. 1. The experimental setup in Fig. 1 is modified accordingly when the 800-nm laser illumination was used; the lenses L1, L2 and the water are removed and the rest of the setup is reserved. Both the maximum resolvable spatial frequencies of the images obtained using these two illumination sources are 45.3 lp/mm, which corresponds to a spatial resolution of ~11.05 μm. Then, we image the target patterns in a scattering environment with an optical depth (OD) of 11. OD is defined as $-\ln(I/I_0)$, where I is the intensity of the ballistic light exiting the scattering medium and I_0 is the intensity of the light entering the scattering medium. A suspension of 3.13-μm-diameter polystyrene spheres is used as the scattering medium. The images obtained using the 800-nm femtosecond laser and SC illuminations are shown in Figs. 2(c) and 2(d), respectively. Speckles are clearly visible in Fig. 2(c) and cause an intense noise, corrupting the images significantly. The effects of laser speckle in the images presented in Fig. 2(d) are significantly mitigated compared to those in Fig. 2(c). Speckle is usually characterized by the speckle contrast C, which is usually expressed as $C \propto 1/\delta\lambda$, where

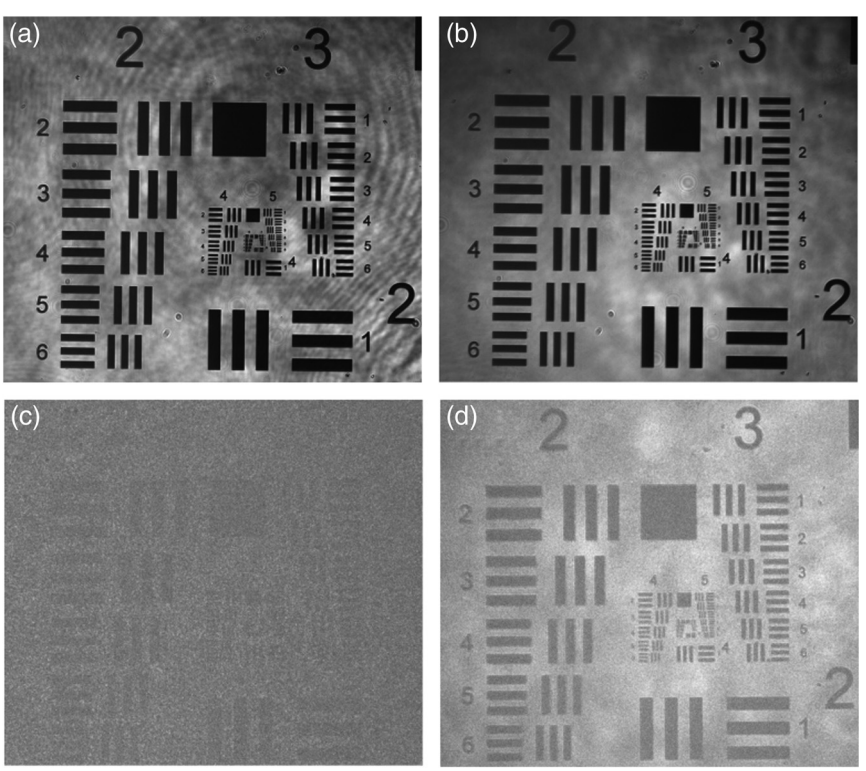

Fig. 2 Images of the object obtained (a) using 800-nm laser and (b) SC illumination without scattering medium. Images of the object obtained (c) using 800-nm laser and (d) SC illumination in a scattering environment.

Downloaded From: https://www.spiedigitallibrary.org/journals/Optical-Engineering on 5/7/2018 Terms of Use: https://www.spiedigitallibrary.org/terms-of-use

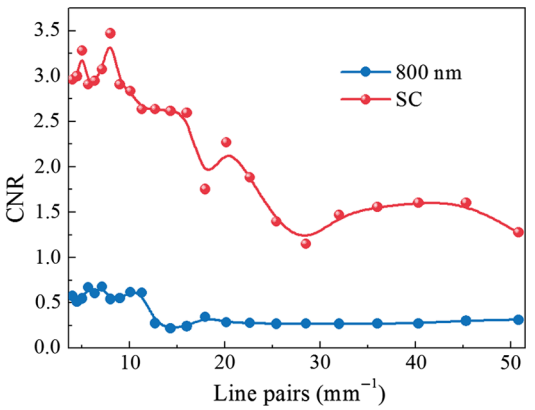

Fig. 3 CNR of the images shown in Fig. 2 versus spatial frequency, which are obtained using the 800-nm laser and SC illuminations in a scattering environment.

$\delta\lambda$ is the wavelength bandwidth of the illumination source.[26] So the speckles in the photographs are suppressed using SC illumination because of its spectral broadening. To quantitatively characterize the qualities of images presented in Figs. 2(c) and 2(d), we calculate the contrast-to-noise ratio (CNR), which describes the identifiability of a feature of interest against a given background as shown in Fig. 3. The CNR is defined as $(\langle I_A\rangle - \langle I_B\rangle)/[(\sigma_A + \sigma_B)/2]$, where I_A and I_B are the intensities of signal-producing structures A and B in the region of interest (for example, a bar in a test pattern and its surrounding background) and σ is the standard deviation of the pixel intensity. When the CNR approaches unity, the image noise is comparable to the feature contrast. Thus, structures are unidentifiable if the CNR is <1. We define the CNR to be 0 if the structures of the object are totally invisible. The CNR for the 800-nm laser illumination is <1 across the entire measured spatial frequency range because of speckle noise. On the other hand, the CNR values of the images obtained using the SC illumination are greater than unity.

We apply the SC illumination to explore the near-nozzle region of high-pressure diesel sprays as described in Fig. 1. First, for comparison, images of the fuel spray captured using the 800-nm laser and SC illuminations are presented in Figs. 4(a) and 4(b), respectively. At $d = 140$ μm, the fuel spray is injected into ambient air with P_r of 600 bar. Speckles are clearly visible on the periphery of the fuel spray core in Fig. 4(a), leading to the information distortion for gas–fuel interfaces in the shadowgraphs. It is difficult to identify the microstructures, such as droplets and filaments, in the images obtained using the 800-nm laser illumination. From Fig. 4(b), we can see that the effects of laser speckle in the spray images obtained using the SC illumination are significantly mitigated, and explicit morphology of the gas–fuel interfaces is imaged in the shadowgraphs. Compared with the 800-nm laser illumination, the SC illumination shows increased ability to identify small-scale liquid structures on the periphery of the spray. The small structures in early spray development are crucial in determining the sizes of the droplets that break from these structures.

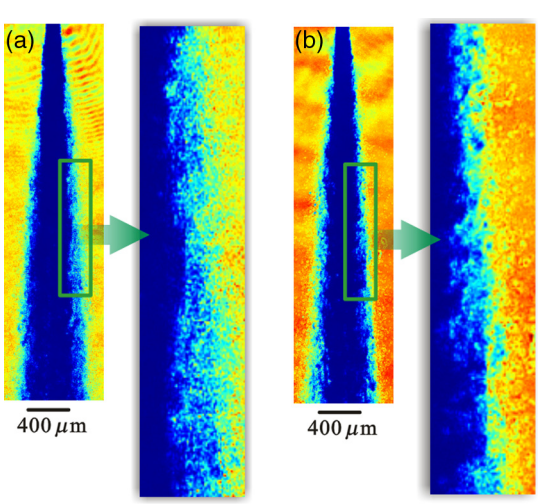

Fig. 4 Images of the fuel spray captured using (a) 800-nm laser illumination and (b) SC illumination.

The theoretical fuel velocity estimated from Bernoulli's equation is on the order of 250 m/s for a P_r of 600 bar. To prevent motion blur, liquid fuel must travel a distance shorter than a pixel size (i.e., 4.6 μm), corresponding to a travel time of 0.02 μs. The pulse width of the SC is measured to be about 1.5 ps. Displacement of the fuel in the pulse duration of the SC is only 0.375 nm, which is much shorter than the pixel size. Therefore, imaging using the SC illumination has the ability to avoid producing motion blurring for imaging high-pressure fuel spray.

In what follows, the morphology of the fuel spray is investigated using the SC illumination imaging method, in which the d ranges from 80 to 180 μm. And we modify P_r from 200 to 1200 bar with 200-bar gradient under each nozzle diameter condition. The images of the fuel spray with d of 80, 100, 120, 140, and 180 μm are presented in Figs. 5(a)–5(e), respectively. The images are arranged from left to right according to the injection pressure in each subgraph. At $d = 80$ μm, the jet is columnar with surface instabilities that grow downstream to where it has a twisted appearance at low P_r. When P_r increases, some surface structures, such as lobes and drops, can be seen to be ejected from the jet. At $d = 100$ μm, surface lobes and bridges are generated at low P_r. Many drops, bridges, and ligaments are stripped from the twisted liquid core, and the jet's spanwise dimension noticeably grows away from the injector exit lane with the increase of P_r. At $d = 120$ μm, drastic changes in the details of the interface are seen even at $P_r = 200$ bar. More surface structures, especially droplets, sputter in the near-nozzle filed of the fuel spray with increasing the pressure. When P_r increases to 1000 bar, a lot of droplets are generated to envelop the liquid core and the other structures appear rarely in the shadowgraphs. At $d = 140$ μm, the development of the structures of spray according to P_r is similar to that at $d = 120$ μm. It should be noted that there are a few holes in the center of liquid core at low P_r under this d condition. When d is increased to 180 μm, at low P_r, the liquid core appears fluffy because of plenty of holes in the center. The droplets are thicken with the increase of P_r until at $P_r = 600$ bar when all the holes are filled by the dense droplets. With the SC illumination, the clarity features in the near-nozzle field of spray were imaged to study the precursors to droplet and spray formations under different injection conditions. The ballistic light attenuates because of scattering of dense droplets. Under

Downloaded From: https://www.spiedigitallibrary.org/journals/Optical-Engineering on 5/7/2018 Terms of Use: https://www.spiedigitallibrary.org/terms-of-use

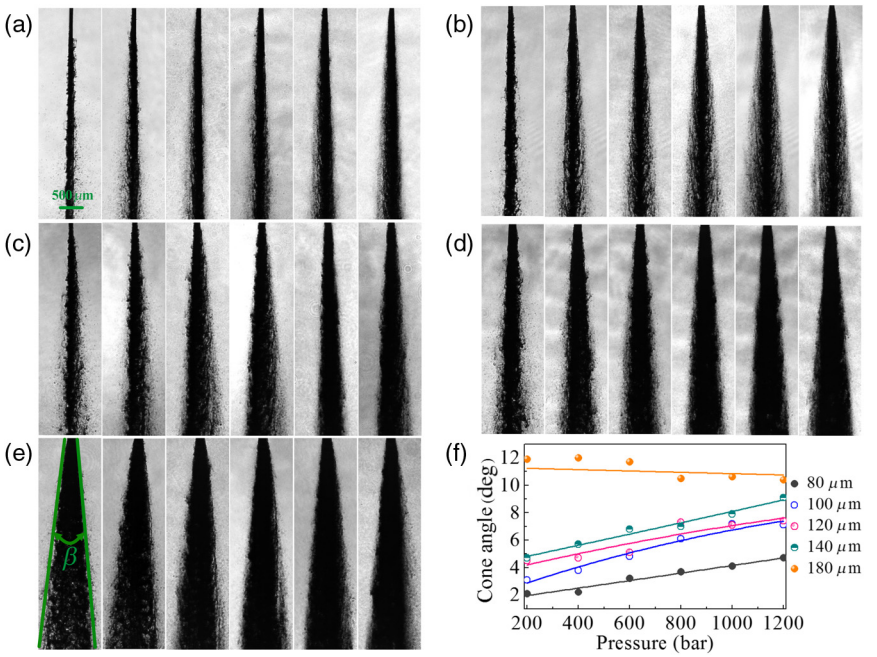

Fig. 5 (a)–(e) Images of the fuel spray captured using the SC illumination. The d for the spray are 80, 100, 120, 140, and 180 μm, respectively, and the P_r is modified arranging from left to right corresponding to 200, 400, 600, 800, 1000, and 1200 bar, respectively, for each d value. (f) Effect of the injection pressure on spray cone angle for nozzles having different d values.

some injection conditions, the microstructures, such as holes, filled by the dense droplets may not be observed in the shadowgraphs if the power of the SC illumination is not high enough. In this case, the power of the femtosecond laser should be increased to enhance the SC, or the conversion efficiency of SC generation should be improved.

The fuel spray cone angle is usually employed to characterize the spray. The cone angle β is formed by two tangent lines originating from the injector tip and passing through the maximum radial positions of the two sides of the spray, as shown in the leftmost subgraph of Fig. 5(e). Figure 5(f) shows the influence of liquid injection pressure on the spray cone angle for nozzles having different orifice diameters. The spray cone angle increases with P_r for d ranges from 80 to 140 μm. At $d = 180$ μm, there is no noticeable influence of injection pressure on the spray angle. It is apparent that the spray cone angle changes with increase in injection pressure depending on the orifice geometry. The similar conclusion was reported in the earlier literature.[27] However, in Varde's work, a xenon lamp with controlled flash duration that is longer than 100 ns is used as the illumination source to capture the shadowgraph of diesel spray. Using this method, the microstructures in the near-nozzle region cannot be observed in the shadowgraph because of motion blurring effects. Due to the temporal ultrashort pulse width of SC, clarity images of the microstructures, i.e., lobes, holes, ligaments, and bridges, can be acquired using SC illumination.

4 Conclusions

In conclusion, we employ SC illumination to image high-pressure fuel sprays in the near-nozzle region. The disturbance of speckles in the images of spray in the near-nozzle region is significantly mitigated using SC illumination and the identifiability of the microstructures in the spray was meaningfully improved. From the images captured using SC illumination under different injection conditions, we acquire the clear images of surface features and the influence of the orifice dimensions on spray cone angle of the sprays as well as on the fuel pressures.

Acknowledgments

The authors gratefully acknowledge the financial support for this work provided by the National Natural Science Foundation of China under the Grant Nos. 61427816 and 61690221. Collaborative Innovation Center of Suzhou Nano Science and Technology also supported this work.

References

1. D. Jarrahbashi et al., "Early spray development at high gas density: hole, ligament and bridge formations," *J. Fluid Mech.* **792**, 186–231 (2016).
2. O. A. Kuti et al., "Characterization of spray and combustion processes of biodiesel fuel injected by diesel engine common rail system," *Fuel* **104**, 838–846 (2013).
3. S. Moon et al., "Near-field dynamics of high-speed diesel sprays: effects of orifice inlet geometry and injection pressure," *Fuel* **133**, 299–309 (2014).
4. J. Manin et al., "Microscopic investigation of the atomization and mixing processes of diesel sprays injected into high pressure and temperature environments," *Fuel* **134**, 531–543 (2014).
5. Z. Wang et al., "Ultra-high speed imaging study of the diesel spray close to the injector tip at the initial opening stage with split injection," *Appl. Energy* **163**, 105–117 (2016).
6. W. Huang, S. Moon, and K. Ohsawa, "Near-nozzle dynamics of diesel spray under varied needle lifts and its prediction using analytical model," *Fuel* **180**, 292–300 (2016).
7. Z. Wu, Z. Zhu, and Z. Huang, "An experimental study on the spray structure of oxygenated fuel using laser-based visualization and particle image velocimetry," *Fuel* **85**, 1458–1464 (2006).
8. T. D. Fansler and S. E. Parrish, "Spray measurement technology: a review," *Meas. Sci. Technol.* **26**(1), 012002 (2015).
9. H. Purwar et al., "Ultrafast high-repetition imaging of fuel sprays using picosecond fiber laser," *Opt. Express* **23**(26), 33396–33407 (2015).
10. C. Crua, M. R. Heikal, and M. R. Gold, "Microscopic imaging of the initial stage of diesel spray formation," *Fuel* **157**, 140–150 (2015).
11. O. Liba et al., "Speckle-modulating optical coherence tomography in living mice and humans," *Nat. Commun.* **8**, 15845 (2017).

Downloaded From: https://www.spiedigitallibrary.org/journals/Optical-Engineering on 5/7/2018 Terms of Use: https://www.spiedigitallibrary.org/terms-of-use

12. A. Ozcan et al., "Speckle reduction in optical coherence tomography images using digital filtering," *J. Opt. Soc. Am. A* **24**(7), 1901–1910 (2007).
13. B. Redding, M. A. Choma, and H. Cao, "Speckle-free laser imaging using random laser illumination," *Nat. Photonics* **6**(6), 355–359 (2012).
14. B. Redding et al., "Low spatial coherence electrically pumped semiconductor laser for speckle-free full-field imaging," *Proc. Natl. Acad. Sci. U. S. A.* **112**(5), 1304–1309 (2015).
15. Z. Cui et al., "Speckle suppression by controlling the coherence in laser based projection systems," *J. Disp. Technol.* **11**(4), 330–335 (2015).
16. C. Li et al., "Alcohol-assisted photoetching of silicon carbide with a femtosecond laser," *Opt. Commun.* **282**(1), 78–80 (2009).
17. Y. Ma et al., "An alternative approach for femtosecond laser induced black silicon in ambient air," *Appl. Surf. Sci.* **261**, 722–726 (2012).
18. V. Nguyen et al., "Electron-hole recombination dynamics in carbon nanodots," *Carbon* **95**, 659–663 (2015).
19. B. Nie et al., "Energy scaling of Yb fiber oscillator producing clusters of femtosecond pulses," *Opt. Eng.* **53**(5), 051505 (2017).
20. S. A. Kovalenko et al., "Femtosecond spectroscopy of condensed phases with chirped supercontinuum probing," *Phys. Rev. A* **59**(3), 2369–2384 (1999).
21. G. McConnel et al., "Time-correlated single-photon counting fluorescence lifetime confocal imaging of decayed and sound dental structures," *J. Microsc.* **225**(2), 126–136 (2007).
22. J. Barrick et al., "High-speed and high-sensitivity parallel spectral-domain optical coherence tomography using a supercontinuum light source," *Opt. Lett.* **41**(24), 5620–3562 (2016).
23. M. Nakazawa et al., "Coherence degradation in the process of supercontinuum generation in an optical fiber," *Opt. Fiber Technol.* **4**(2), 215–223 (1998).
24. Y. Zheng et al., "Ballistic imaging through an intense scattering medium using a supercontinuum with a roundabout spatial gate," *Opt. Express* **25**(17), 20431 (2017).
25. Y. Zheng et al., "Speckle-suppressed full-field imaging through a scattering medium using a supercontinuum," *Opt. Express* **24**(23), 26338–26343 (2016).
26. J. W. Goodman, *Speckle Phenomena in Optics: Theory and Applications*, Roberts & Co. Publishers, Englewood, Colorado (2009).
27. K. S. Varde, "Spray cone angle and its correlation in a high pressure fuel spray," *Can. J. Chem. Eng.* **63**(2), 183–187 (1985).

Yipeng Zheng is a doctoral candidate at Xi'an Jiaotong University. He received his BS degree in physics from Lanzhou University in 2011 and his MS degree in optics from the Normal University of South China in 2014. His current research interests include ultrafast optics and nonlinear optics.

Biographies for the other authors are not available.

Downloaded From: https://www.spiedigitallibrary.org/journals/Optical-Engineering on 5/7/2018 Terms of Use: https://www.spiedigitallibrary.org/terms-of-use